
IMPACT OF SEED NODE POSITION ON NETWORK ROBUSTNESS UNDER LOCALIZED ATTACKS

Masaki Chujo, Shu Liu, Fujio Toriumi

Department of Systems Innovation, School of Engineering

The University of Tokyo

Tokyo Japan

mchujo@g.ecc.u-tokyo.ac.jp

ABSTRACT

Localized attacks (LAs), where damage propagates from a single seed node to its neighbors, pose significant threats to the robustness of complex networks. Although previous studies have extensively analyzed network vulnerability under such attacks, they typically assume random seed node placement and evaluate average robustness. However, the structural position of the seed node can significantly impact the extent of damage. This study proposes the Localized Attack Vulnerability Index (LAVI), a node-level metric that quantifies the potential impact of a LA initiated at a specific node. LAVI quantifies the cumulative number of severed links during attack progression, capturing how local connectivity and topological position amplify the resulting damage. Numerical experiments on synthetic and real-world networks demonstrate that LAVI correlates more strongly with network robustness degradation than standard centrality measures, such as degree, closeness, and betweenness. Our findings highlight that classical centrality metrics fail to capture key dynamics of spatially localized failures, while LAVI provides an accurate and generalizable indicator of node vulnerability under such disruptions.

Introduction

Modern societies increasingly depend on large-scale interconnected infrastructures, such as transportation and power grids, whose resilience to spatially concentrated disruptions from natural disasters poses a critical challenge [1, 2, 3, 4, 5, 6]. Addressing this challenge requires models that systematically capture how localized damage can escalate into large-scale systemic failures. To model these dynamics, researchers have investigated localized attacks (LAs) on complex networks, where nodes are sequentially removed based on their topological or spatial proximity to a designated seed node [7, 8, 9, 10]. These models are inspired by real-world phenomena, such as earthquakes, floods, and other spatially concentrated disruptions, where damage typically originates at a single point and spreads locally [9, 11, 12].

Extensive research on network vulnerability under LAs has shown that even small initial disruptions can trigger abrupt fragmentation or cascading failures [7, 13, 8, 14, 15]. Recent studies have examined how network properties, such as degree distribution, clustering, community structure, and degree correlations, influence robustness to LAs, and have proposed mitigation strategies, including structural rewiring, localized recovery, and selective protection [10, 16, 17, 18, 19, 20].

These theoretical insights are supported by empirical studies demonstrating that even modest localized disruptions can induce large-scale failures in spatial infrastructure systems, such as road networks and power grids [21, 22, 23, 24, 12]. For instance, empirical analyses of post-earthquake road networks have revealed that the removing a few critical links in a localized region can severely degrade overall connectivity [23]. Similarly, studies have demonstrated that localized flooding, despite its limited spatial scope, can trigger cascading failures in transportation networks owing to load redistribution and compound disruptions [24, 12]. These findings highlight that the spatial concentration of initial damage, rather than its overall size, often determines systemic impact. Therefore, understanding the conditions under which localized damage escalates to network-wide failures is essential for designing resilient infrastructure systems.

Related efforts have also investigated node importance and dynamic processes in complex networks [25, 26]. In the context of targeted attacks, it is well-known that targeted removal of nodes in descending order of degree or betweenness centrality can rapidly fragment networks and significantly reduce global connectivity [27, 28]. Such strategies have therefore been widely used as benchmarks for assessing network robustness. Beyond classical centrality heuristics, a variety of optimization-based frameworks have been developed to identify structurally critical nodes for network dismantling and fragmentation, including optimal percolation [29], belief-propagation-based dismantling [30], and machine-learning-driven network disintegration methods [31]. In parallel, in the context of cascading failures, several studies have reported strong correlations between node centrality measures and failure propagation severity and proposed centrality-based or hybrid strategies to identify critical nodes [32, 33]. Moreover, related optimization and evolutionary approaches have also been explored for influence maximization and diffusion-oriented seed selection problems, aiming to identify influential and robust spreaders under information propagation models [34, 35].

However, despite these advances, most existing approaches implicitly assume global attack or information propagation scenarios in which damage or influence can be applied arbitrarily across the network. In contrast, LAs are inherently constrained by spatial or topological proximity and originate from a single seed node, from which damage propagates outward. Consequently, the mechanisms governing damage amplification under LAs exhibit substantially different characteristics from those underlying classical targeted attack and influence maximization frameworks.

Under such localized propagation dynamics, the position of the seed node is expected to be a key factor in shaping the resulting disruption pattern. In spatially embedded networks, for example, attacks initiated near the topological core may induce substantially more severe damage than those starting from peripheral regions. Nevertheless, most previous LA studies assume random seed selection and evaluate robustness based on averaged realizations [7, 13], thereby obscuring node-specific vulnerability differences and leaving the role of individual seed nodes largely unexplored. While nodes with high degree, closeness, or betweenness centrality have been widely regarded as critical targets in classical targeted attack scenarios, it remains unclear whether these conventional measures are sufficient to characterize vulnerability when damage propagates outward from a single localized seed. This gap suggests that seed-level vulnerability under LAs represents a fundamentally different problem from traditional centrality-based critical node identification and motivates the development of dedicated evaluation metrics.

Therefore, we introduce the Localized Attacks Vulnerability Index (LAVI), a metric designed to quantify the potential damage caused when a specific node acts as the seed of an LA. LAVI measures the extent of link removal resulting from such an attack, providing a proxy for the network's susceptibility to localized disruptions. Extensive numerical simulations show that LAVI correlates substantially more strongly with actual damage than standard centrality metrics. Moreover, conventional measures often fail to explain vulnerability patterns under LAs, indicating that these dynamics are not fully captured by existing frameworks. This highlights the need for new evaluation metrics, such as LAVI, to advance our understanding of network robustness under LAs.

Materials and methods

To evaluate how a seed node's position influences the severity of a LA, we conducted numerical experiments on both synthetic and real-world networks. This section describes the attack model, introduces the proposed vulnerability index, and details the methodological framework for evaluating network robustness under various conditions.

Localized Attack and Robustness Index

To quantitatively evaluate network robustness under LA, we adopted the global robustness index R , which measures the network's ability to maintain connectivity during the node removal process [36, 16]. It is defined as the normalized cumulative size of the largest connected component (LCC):

$$R = \frac{1}{N} \sum_{q=1}^N s_{\text{LA}}(q), \quad (1)$$

where N is the total number of nodes in the original network, and $s_{\text{LA}}(q)$ denotes the relative size of the LCC after the removal of q nodes under LA.

The LA model simulates damage spreading from a local region within the network. The procedure begins by selecting a seed node uniformly at random as the attack center, after which nodes are removed sequentially in layer based on their shortest-path distance l from the seed. Specifically, shell $l = 0$ contains the seed node itself, $l = 1$ includes its immediate neighbors. Nodes are removed in random order within each shell, and the process continues outward until q nodes have been removed.

After each removal step, the LCC is computed, and its size normalized by N yields $s_{\text{LA}}(q)$, representing the fraction of nodes remaining in the LCC. A higher R value indicates greater robustness, reflecting the network's ability to maintain LCCs throughout the attack. This measure provides a comprehensive assessment of resilience to spatially localized failures.

It should be noted that our analysis focuses on structural robustness based on network connectivity and does not explicitly consider flow dynamics, capacity constraints, or domain-specific performance measures. Although real-world networks involve diverse operational mechanisms, maintaining basic connectivity between nodes is generally a necessary prerequisite for functional operation. For this reason, the size of the LCC has been widely used as a proxy for functional connectivity in network robustness studies [36, 16]. In this study, we therefore evaluate network robustness under localized attacks by examining how the size of the LCC evolves during the attack process.

Localized Attack Vulnerability Index for a Seed Node

To quantify the influence of a seed node i on severity of a LA in $G = (V, E)$, we introduce the LAVI $\mathcal{L}(i)$. This metric is based on the cumulative number of half-links severed as the attack progresses through concentric distance shells, where each undirected edge contributes two half-links (one per endpoint).

First, we compute the shortest-path distances from the seed node i using a breadth-first search:

$$d_i(v) = \text{dist}_G(i, v), \quad v \in V.$$

Let $d_{\max} = \max_{v \in V} d_i(v)$ be the maximum distance. For each distance $d \in \{0, 1, \dots, d_{\max}\}$, we define the shell

$$S_d = \{v \in V : d_i(v) = d\}.$$

Therefore, we construct the removal sequence

$$\pi(i) = [S_0, S_1, \dots, S_{d_{\max}}],$$

by concatenating shells in non-decreasing order of distance from the seed node i . Within each shell S_d , nodes are processed based on two ordering schemes:

- **Random-case removal:** nodes are randomly shuffled using a fixed random seed for reproducibility, yielding a uniformly random permutation.
- **Worst-case removal:** nodes are sorted in descending order of their original degrees $\deg_G(v)$, such that high-degree nodes are deactivated first.

These two schemes represent different types of localized disruption scenarios. The random-case models stochastic local damage processes, such as those induced by natural hazards, where the internal failure order within an affected region is uncertain. In contrast, the worst-case removal approximates adversarial localized attacks that preferentially target structurally important nodes, providing an upper bound on potential damage severity.

Let $\pi(i) = (v_1, v_2, \dots, v_{|V|})$ denote the full node removal sequence, ordered such that nodes closer to the seed i are removed earlier. After removing each node v_i , we track the cumulative number of half-links severed up to step k as

$$C_k = \sum_{i=1}^k \deg_G(v_i), \quad k = 1, \dots, |V|.$$

The LAVI $\mathcal{L}(i)$ is defined as

$$\mathcal{L}(i) = \frac{1}{|V|} \sum_{k=1}^{|V|} C_k = \frac{1}{|V|} \sum_{k=1}^{|V|} (|V| - k + 1) \deg_G(v_k).$$

The complete procedure for computing $\mathcal{L}(i)$ is summarized in Table 1.

Intuitively, $\mathcal{L}(i)$ is proportional to the area under the curve of cumulative half-link removals versus the removal index; a larger $\mathcal{L}(i)$ indicates that more links are removed at earlier stages of the attack process, reflecting more severe damage initiated from the seed node i . This design is motivated by the fact that network connectivity generally becomes more fragile as links are removed, and substantial early link loss under localized attacks tends to accelerate large-scale fragmentation. Unlike conventional centrality measures that capture static structural importance, $\mathcal{L}(i)$ explicitly reflects the dynamic accumulation of connectivity loss during the outward propagation of localized failures. An illustrative 3×3 grid example is shown in Fig. 1 to visualize the cumulative half-link removal process underlying $\mathcal{L}(i)$.

Table 1: Pseudo-code for computing the LAVI.

Input:	Undirected graph $G = (V, E)$, seed node $i \in V$
Parameter:	ordering mode $\in \{\text{random, worst}\}$
Output:	LAVI value $\mathcal{L}(i)$
Step	Procedure
1	Compute shortest-path distances $d_i(v)$ from i to all $v \in V$ using BFS.
2	Group nodes by distance and construct the ordered list $\pi(i) = [S_0, S_1, \dots, S_{d_{\max}}]$.
3	If mode is random , randomly permute nodes within each S_ℓ .
4	If mode is worst , sort nodes within each S_ℓ in descending order of degree $\deg_G(v)$.
5	Flatten $\pi(i)$ into a sequence $(v_1, v_2, \dots, v_{ V })$ and initialize $C_0 \leftarrow 0$.
6	For $k = 1, 2, \dots, V $, update $C_k \leftarrow C_{k-1} + \deg_G(v_k)$.
7	Compute $\mathcal{L}(i) = \frac{1}{ V } \sum_{k=1}^{ V } C_k$.
8	Return $\mathcal{L}(i)$.

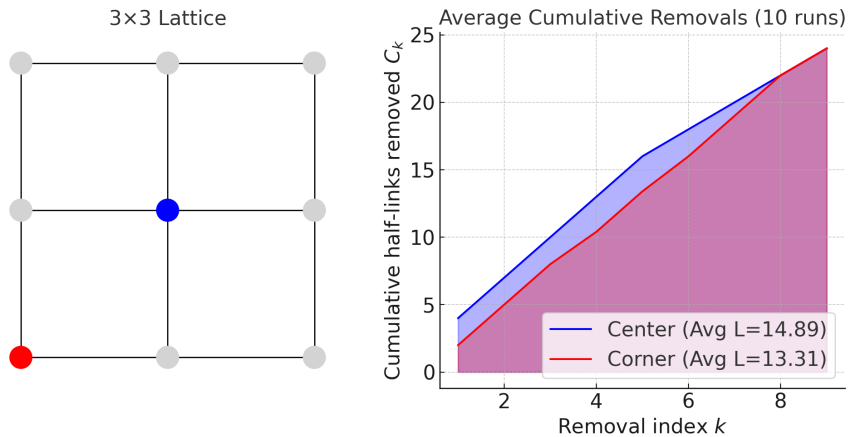


Figure 1: Random-case cumulative half-link removals C_k versus removal index k on a 3×3 lattice. The blue curve shows the average over 10 runs when the seed node is placed at the center, while the red curve corresponds to placement at a corner. The shaded areas under each curve correspond to the LAVI $\mathcal{L}(i)$. A larger shaded area (center seed) indicates more rapid link removal and hence greater vulnerability.

Note that dividing $\mathcal{L}(i)$ by $2M$ yields a normalized value in the range $[0, 1]$; however, we intentionally avoid this normalization, as it tends to excessively compress the values in sparse networks and reduce discriminative resolution among seed nodes.

The computation of $\mathcal{L}(i)$ consists of (i) breadth-first search for distance calculation in $O(|V| + |E|)$ time; (ii) shell construction in $O(|V|)$; (iii) within-shell ordering, requiring $O(|V| \log |V|)$ time in the worst-case removal (assuming worst-case shell size), or $O(|V|)$ time in the random-case removal via random shuffling; and (iv) cumulative sum calculation in $O(|V|)$. The total time complexity is $O(|V| \log |V| + |E|)$ for worst-case removal and $O(|V| + |E|)$ for random-case removal.

Results

To evaluate how the structural position of a seed node affects the outcome of LAs, we performed simulations on both synthetic and real-world networks. Synthetic networks enable controlled variation of structural properties, while real-world networks demonstrate the applicability of our findings to practical systems. The results are presented in two parts: first for synthetic networks, then for real-world datasets.

Results for Synthetic Networks

To investigate the relationship between network structure and vulnerability to LAs, we performed a systematic analysis using the Barabási–Albert (BA) model [37], a widely used generative model for scale-free networks. Specifically,

Table 2: Spearman and Pearson correlations between robustness index R and node-level indices in BA networks of varying sizes ($N = 100, 1000, 10000, m = 2$). Bold indicates the strongest (most negative) correlation for each network.

Network	Index	Spearman	Pearson
$N = 100$	LAVI(random)	-0.913	-0.900
	LAVI(worst)	-0.818	-0.788
	Degree	0.140	0.043
	Closeness	0.043	0.082
	Betweenness	0.037	0.036
$N = 1000$	LAVI(random)	-0.693	-0.717
	LAVI(worst)	-0.663	-0.692
	Degree	-0.031	-0.033
	Closeness	-0.009	-0.083
	Betweenness	-0.081	-0.062
$N = 10000$	LAVI(random)	-0.570	-0.590
	LAVI(worst)	-0.464	-0.488
	Degree	-0.033	0.013
	Closeness	0.181	0.138
	Betweenness	0.062	0.023

we generated BA networks with $N = 100$ nodes and attachment parameter $m = 2$, yielding sparse yet connected topologies with heterogeneous degree distribution.

We analyzed the impact of LAs initiated from different seed nodes by randomly sampling 100 seed nodes from the network. For each sampled seed, we conducted 100 independent simulations of LA and computed the average robustness index R . This procedure yields a stable quantification of the structural damage associated with attacks initiated from various topological positions.

To understand which node-level properties are most indicative of vulnerability, we computed two versions of the proposed LAVI: $\mathcal{L}_{\text{worst}}$ and $\mathcal{L}_{\text{random}}$, along with classical centrality measures, including degree, closeness, and betweenness centrality [38].

Figure 2 presents the correlations between the robustness index R and various node-level metrics. The top row displays results for the two vulnerability indices and their mutual correlation, while the bottom row displays correlations with the three centrality measures.

The top row results show that both vulnerability indices are strongly negatively correlated with robustness. Higher values of $\mathcal{L}_{\text{random}}$ and $\mathcal{L}_{\text{worst}}$ are associated with lower values of R , indicating that seed nodes causing faster cumulative link removals tend to cause greater structural damage. Among them, $\mathcal{L}_{\text{random}}$ shows the strongest correlation (Spearman $\rho = -0.913$, Pearson $r = -0.900$), followed by $\mathcal{L}_{\text{worst}}$ (Spearman $\rho = -0.818$, Pearson $r = -0.788$). The high agreement between these two indices (Spearman and Pearson $\rho = 0.927$) indicates that the structural position of the seed node plays a dominant role, irrespective of within-shell removal order.

In contrast, the classical centrality measures (bottom row) show weak or negligible correlations with robustness. Degree centrality exhibits virtually uncorrelated with R , while closeness and betweenness fail to explain robustness variations. These findings suggest that traditional centrality metrics are ineffective in identifying structurally vulnerable nodes under LA scenarios.

Overall, these results highlight the effectiveness of the proposed LAVI $\mathcal{L}(i)$ in identifying seed nodes cause the greatest reduction in robustness. By capturing both the spatial progression of the attack and the rate of link removal, the index provides a more relevant assessment of vulnerability than conventional centrality measures.

To assess the scalability of our findings, we extended the analysis to BA networks with $N = 1000$ and $N = 10000$, using the same attachment parameter $m = 2$. Table 2 summarizes the Spearman and Pearson correlations between R and the various node-level indices for each network size.

Across all network sizes, both versions of the vulnerability index, especially $\mathcal{L}_{\text{random}}$, maintain strong negative correlations with robustness. However, as the network size increases, these correlations gradually weaken—for example, the Spearman correlation of $\mathcal{L}_{\text{random}}$ with R drops from -0.91 at $N = 100$ to -0.57 at $N = 10000$. Therefore, while LAVI remains a reliable predictor of vulnerability, its ability to differentiate may decline in larger, more heterogeneous networks, where local effects weaken.

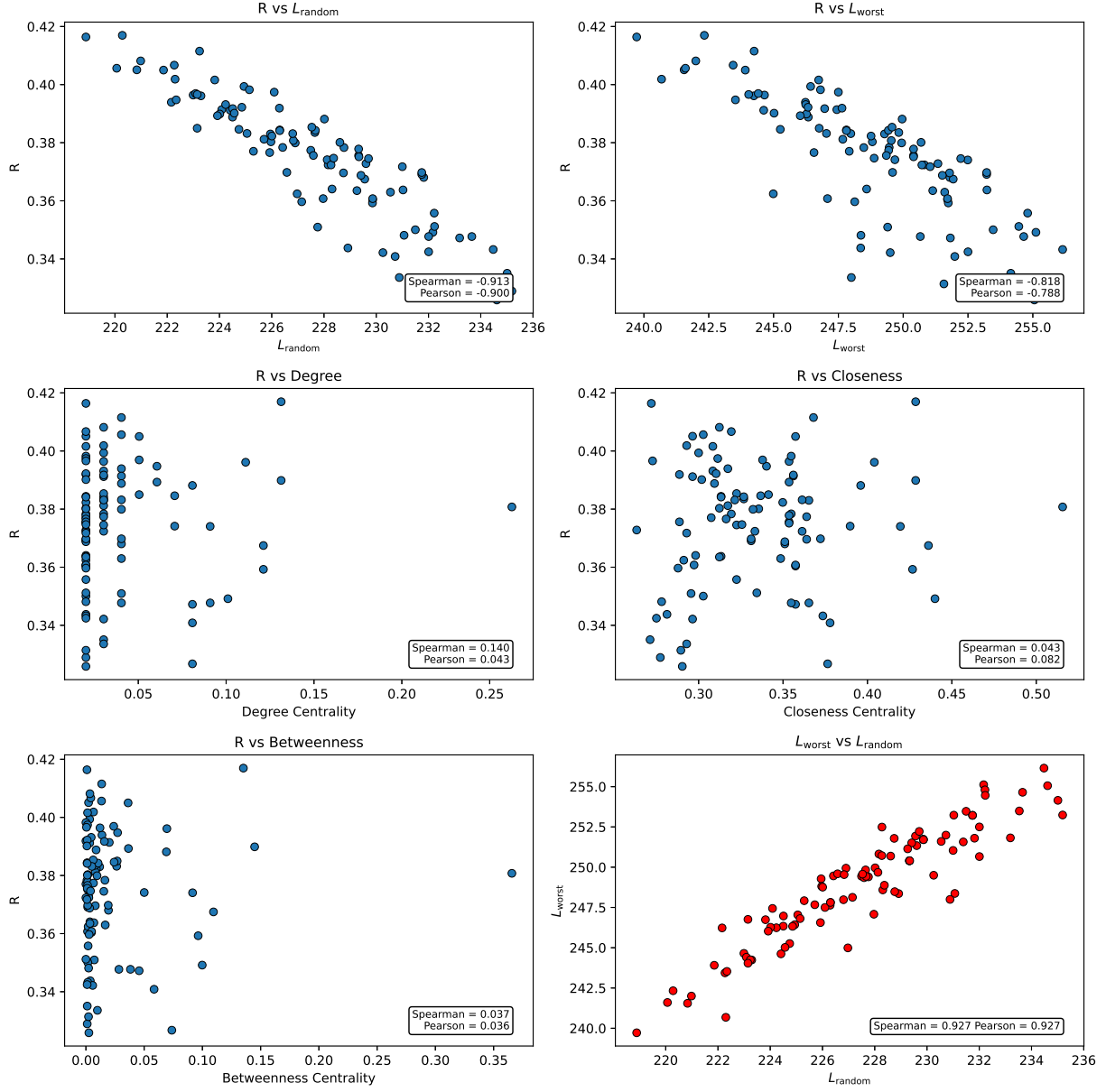


Figure 2: Correlation between the robustness index R and various indices characterizing the choice of the seed node in a Barabási-Albert network with $N = 100$ and $m = 2$. The panels show correlations between R and $\mathcal{L}_{\text{random}}$, $\mathcal{L}_{\text{worst}}$, degree, closeness, and betweenness centrality of the seed node, as well as the mutual correlation between $\mathcal{L}_{\text{worst}}$ and $\mathcal{L}_{\text{random}}$. Spearman and Pearson correlation coefficients are reported in each panel.

Table 3: Summary statistics of the real-world networks used in the analysis.

Network Name	Type	#Nodes	#Edges	Assortativity	Reference
NCI1_g4094	Cheminformatics	90	98	-0.286	[39]
inf-USAir97	Infrastructure	332	2126	-0.208	[39, 40]
power-494-bus	Power grid	494	586	-0.074	[39]
bio-diseasome	Biological	516	1188	0.067	[39, 41]
fb-pages-food	Social	620	2102	-0.028	[39, 42]
bio-yeast	Biological	1458	1948	-0.210	[39, 43]
inf-openflights	Infrastructure	2939	15677	0.051	[39, 44]

Table 4: Spearman correlations between the robustness index R and seed node indices. Values in parentheses are p-values. Bold shows the strongest correlation.

Network	LAVI(worst)	LAVI(random)	Degree	Closeness	Betweenness
NCI1_g4094	-0.90 (5.9e-33)	-0.60 (4.0e-10)	0.03 (7.6e-01)	-0.70 (1.4e-14)	-0.16 (1.3e-01)
inf-USAir97	-0.42 (1.3e-05)	-0.58 (1.9e-10)	0.02 (8.8e-01)	-0.22 (2.6e-02)	-0.09 (3.6e-01)
power-494-bus	-0.85 (3.2e-29)	-0.81 (2.8e-24)	-0.11 (2.6e-01)	-0.48 (3.8e-07)	-0.08 (4.2e-01)
bio-diseasome	-0.10 (3.1e-01)	0.20 (5.0e-02)	-0.01 (9.3e-01)	-0.31 (2.0e-03)	-0.26 (1.0e-02)
fb-pages-food	-0.56 (1.3e-09)	-0.50 (9.4e-08)	0.15 (1.5e-01)	-0.20 (5.1e-02)	0.00 (9.9e-01)
bio-yeast	-0.75 (3.2e-19)	-0.63 (2.7e-12)	0.03 (7.7e-01)	-0.16 (1.1e-01)	0.07 (5.1e-01)
inf-openflights	-0.53 (1.5e-08)	-0.42 (1.2e-05)	0.20 (4.3e-02)	-0.01 (9.3e-01)	0.20 (4.4e-02)

In contrast, classical centrality measures consistently yield weak or negligible correlations across all scales. Therefore, these results further elaborate that the proposed vulnerability indices outperform traditional measures in identifying structurally critical nodes under LAs. This phenomenon holds across different network sizes.

Results for Real-World Networks

To assess the practical relevance of our findings, we performed LA analysis to seven real-world networks drawn from diverse domains, including infrastructure, biological systems, social networks, and cheminformatics. The datasets, listed in Table 3, vary widely in size, density, and assortativity. This enables easy examination of the generality of the proposed vulnerability indices under heterogeneous conditions.

Figure 3 presents results for one representative case, the power-494-bus network. The top row confirms that both $\mathcal{L}_{\text{worst}}$ and $\mathcal{L}_{\text{random}}$ are strongly negatively correlated with the robustness index R , which is consistent with our findings in BA synthetic networks. The bottom row indicates that traditional centrality measures, degree, closeness, and betweenness, exhibit negligible or weak associations with robustness.

To systematically compare across all real-world networks, Tables 4 and 5 report Spearman and Pearson correlations between the robustness index R and the node-level indices. In most cases, $\mathcal{L}_{\text{worst}}$ exhibits the strongest (most negative) correlation with robustness, highlighting its effectiveness as a predictor of vulnerability under LA. $\mathcal{L}_{\text{random}}$ performs well, often outperforming traditional centrality measures despite not being optimized for worst-case shell removal.

This overall trend mirrors the results from the synthetic BA model, indicating that the predictability of the proposed indices generalizes well to real-world systems. However, certain exceptions emerge, as in networks such as bio-diseasome, where LAVI exhibits only a weak correlation with robustness (approximately -0.1). To further investigate this behavior, Fig. 4 presents a representative example from the bio-diseasome network, in which two seed nodes, A and B, exhibit nearly identical $\mathcal{L}_{\text{random}} = 1344$ and 1336 , while their robustness indices under localized attacks differ substantially ($R_{\text{LA}} = 0.34$ and 0.16). Although the cumulative half-link removals remain comparable (Fig. 4(a)), the evolution of the largest connected component shows pronounced differences (Fig. 4(b)), indicating that similar local vulnerability scores do not necessarily translate into equivalent global fragmentation outcomes.

The network visualization in Fig. 4(c) further reveals that node B is located near the network core, whereas node A lies closer to the periphery, and that the network is composed of multiple small clusters bridged by a limited number of inter-community connections. In such topologies, the disruption of bridging links, rather than the total number of removed links, becomes the dominant factor governing large-scale fragmentation. This mechanism is consistent with previous observations suggesting that attacks targeting high-betweenness nodes can, in some cases, outperform degree-based strategies in real-world networks [28]. In networks with modular structure and bridge-dependent connectivity, LAVI may exhibit weaker correlations with robustness, reflecting a structural limitation of the proposed approach.

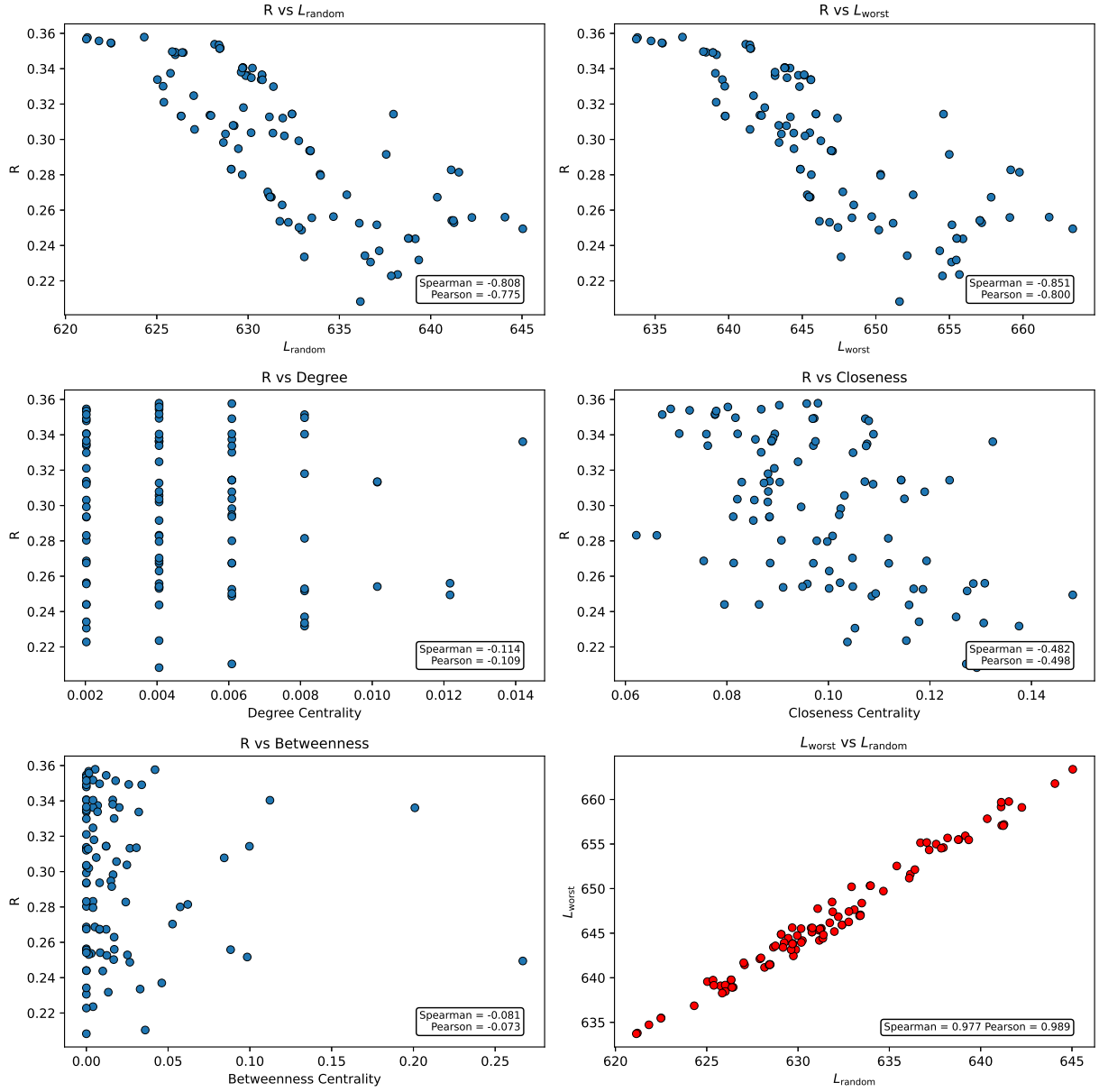


Figure 3: Correlation between the robustness index R and various indices characterizing the choice of the seed node in the power-494-bus network. The panels demonstrate correlations between R and L_{random} , L_{worst} , degree, closeness, and betweenness centrality of the seed node, as well as the mutual correlation between L_{worst} and L_{random} . Spearman and Pearson correlation coefficients are reported in each panel.

These results also help explain why, among conventional centrality measures, closeness centrality exhibits relatively better performance in the bio-diseasome network. As shown in Fig. 4(c), this network is characterized by modular structure and bridge-like connections, where damage propagation strongly depends on the relative position of the seed within the global topology. In such settings, seeds located closer to the network core can more easily affect multiple communities, leading to more severe fragmentation.

In contrast, degree and betweenness centralities primarily capture local connectivity patterns or shortest-path structure, which are effective in classical targeted attack scenarios but less informative for predicting the global impact of expanding localized failures. As a result, conventional centrality measures exhibit limited correlation with robustness

Table 5: Pearson correlations between the robustness index R and seed node indices. Values in parentheses are p-values. Bold shows the strongest correlation.

Network	LAVI(worst)	LAVI(random)	Degree	Closeness	Betweenness
NCI1_g4094	-0.92 (4.7e-37)	-0.73 (4.1e-16)	0.08 (4.6e-01)	-0.75 (1.9e-17)	-0.27 (9.7e-03)
inf-USAir97	-0.59 (8.4e-11)	-0.64 (6.4e-13)	-0.13 (1.8e-01)	-0.37 (1.5e-04)	-0.18 (8.1e-02)
power-494-bus	-0.80 (1.8e-23)	-0.77 (3.1e-21)	-0.11 (2.8e-01)	-0.50 (1.3e-07)	-0.07 (4.7e-01)
bio-diseasome	-0.11 (2.9e-01)	0.11 (2.6e-01)	0.05 (6.4e-01)	-0.37 (1.6e-04)	-0.18 (7.8e-02)
fb-pages-food	-0.66 (6.8e-14)	-0.46 (1.6e-06)	0.05 (6.5e-01)	-0.16 (1.2e-01)	-0.05 (6.3e-01)
bio-yeast	-0.77 (1.6e-20)	-0.67 (2.2e-14)	-0.01 (9.3e-01)	-0.21 (3.7e-02)	-0.02 (8.8e-01)
inf-openflights	-0.98 (1.0e-73)	-0.97 (1.8e-62)	-0.02 (8.3e-01)	-0.48 (3.9e-07)	-0.02 (8.5e-01)

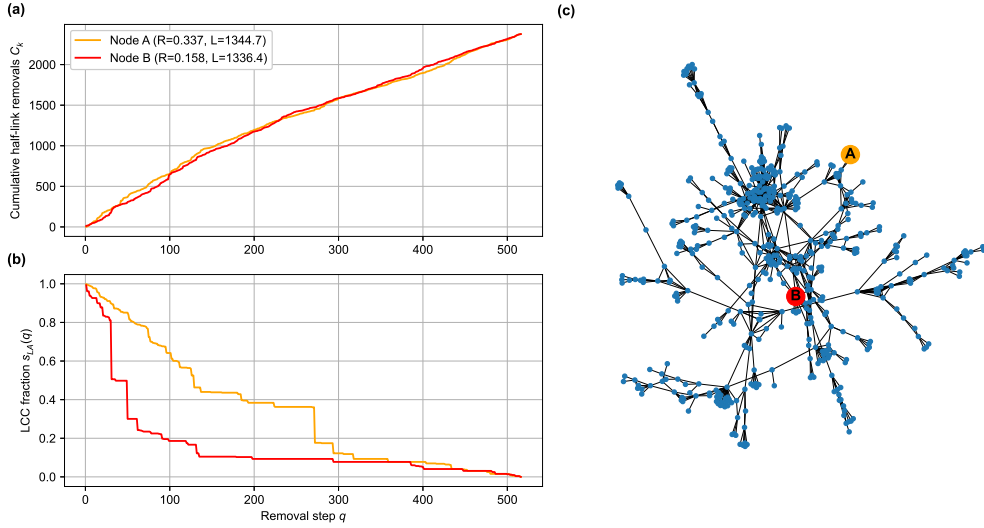


Figure 4: Example from the bio-diseasome network illustrating a case where LAVI fails to distinguish robustness against localized attack. (a) Cumulative half-link removals C_k and (b) largest connected component fraction s_{LA} for two seed nodes with similar LAVI values. (c) Network visualization highlighting the positions of the two seeds.

under localized attacks. These observations highlight the necessity of propagation-aware metrics such as LAVI, which explicitly account for the cumulative and evolving nature of localized attack processes.

Collectively, these results indicate that the proposed vulnerability indices consistently outperform conventional centrality measures across both synthetic and empirical networks, highlighting its effectiveness in identifying critical nodes under LAs.

Discussion

Our analysis reveals that the structural vulnerability of complex networks to LAs is not well captured by conventional centrality values of seed nodes. Although high centrality is presumed to indicate vulnerability, our findings show that degree and betweenness have weak associations with robustness loss under localized disruptions. Closeness centrality exhibited moderate correlations in certain cases, particularly in spatially structured networks, but its performance was inconsistent and inferior to the proposed LAVI.

These findings suggest that node importance under LAs cannot be fully explained by global prominence or shortest-path accessibility alone. Instead, the severity of LA depends on how the removal of a seed node initiates and sustains the breakdown of nearby connectivity. LAVI captures this mechanism by quantifying the cumulative loss of links as the attack expands outward in a shell-wise manner, thereby considering both the spatial progression and the structural exposure of the network.

Furthermore, the superiority of LAVI over standard metrics was consistently observed across both synthetic and real-world networks with diverse topologies. Therefore, LAVI’s advantage does not stem from specific structural features—such as scale-free degree distributions or spatial embedding—but from its alignment with the propagation dynamics inherent to localized failures.

Nevertheless, we observed that LAVI’s performance varies across networks. In certain cases, such as the bio-diseasome network, correlations between node-level indices and robustness were weak. The underlying reasons remain unclear but may be related to complex or heterogeneous structural features not fully captured by node-centric measures. Such cases suggest that local vulnerability can be influenced by meso-scale features, such as modularity or functional clustering, that lie beyond the scope of the current framework. Extending LAVI to consider such structural complexity is a promising direction for future work.

It is important to emphasize that the present study focuses on vulnerability from a structural connectivity perspective and does not explicitly incorporate operational processes such as flow redistribution, capacity saturation, or application-specific performance measures. Although connectivity-based robustness captures essential structural degradation under localized attacks, real-world network functionality often depends on additional dynamic and weighted interaction mechanisms. Extending the proposed framework to incorporate such effects therefore represents an important direction for future research.

From a computational perspective, computing LAVI for a single seed node is relatively efficient, as it mainly relies on a breadth-first search and simple degree-based accumulation. However, applying LAVI to dynamically evolving networks poses additional challenges. In real-time settings where network topology changes frequently, repeated recomputation would be required, which may limit practical deployment. Moreover, the proposed framework assumes access to global network structural information, which may be difficult to obtain in systems where connectivity data are incomplete or distributed. At present, LAVI is therefore most suitable for static or slowly evolving networks, such as pre-disaster infrastructure models, highlighting the need for future extensions toward dynamic and partially observable network settings.

From an applied perspective, LAVI may be useful for identifying locations that are likely to experience severe damage under localized disruptions, such as regions highly exposed to earthquake-induced failures in transportation or utility networks, as well as structurally central regions in criminal or covert networks. By detecting seed nodes whose surrounding regions are particularly vulnerable, the proposed metric can support preventive protection strategies and targeted reinforcement of critical areas. For example, focusing on the localized neighborhoods surrounding nodes with high LAVI values may provide structural guidance for designing interventions to disrupt criminal or covert networks [45], while in infrastructure systems it may help prioritize regions for reinforcement or monitoring to mitigate the impact of localized hazards [23].

Overall, our findings highlight the need to shift in vulnerability analysis toward metrics that explicitly incorporate the spatial and structural dynamics of failure. By linking node importance to the actual dynamics of damage progression, LAVI offers a practical alternative to traditional centrality-based assessments.

Conclusion

This study introduced the Localized Attack Vulnerability Index (LAVI), a node-level metric for assessing the impact of LAs on complex networks. In contrast to conventional centrality measures, LAVI captures the spatial and structural trajectory of damage as it spreads from a seed node.

Simulations on both synthetic and real-world networks show that LAVI is strongly associated with robustness loss under localized disruptions, consistently outperforming classical centrality metrics. These findings highlight the need for vulnerability measures that capture the propagation and accumulation of localized damage, an aspect overlooked by conventional centrality-based approaches.

The findings demonstrate that the position of the seed node, the origin of spatial damage, plays a critical role in determining network robustness. By quantifying this effect, LAVI provides a foundation for assessing the vulnerability of infrastructure systems and informing countermeasures against localized disasters, such as earthquakes and tsunamis.

Acknowledgments

Partial financial support was received from TechnoPro Holdings, Inc.

References

- [1] Boin A, McConnell A. Preparing for critical infrastructure breakdowns: the limits of crisis management and the need for resilience. *Journal of contingencies and crisis management*. 2007;15(1):50–59.
- [2] Mukherjee B, Habib MF, Dikbiyik F. Network adaptability from disaster disruptions and cascading failures. *IEEE Communications Magazine*. 2014;52(5):230–238.
- [3] Khademi N, Balaei B, Shahri M, Mirzaei M, Sarrafi B, Zahabiun M, et al. Transportation network vulnerability analysis for the case of a catastrophic earthquake. *International journal of disaster risk reduction*. 2015;12:234–254.
- [4] Tang P, Xia Q, Wang Y. Addressing cascading effects of earthquakes in urban areas from network perspective to improve disaster mitigation. *International journal of disaster risk reduction*. 2019;35:101065.
- [5] Kilanitis I, Sextos A. Integrated seismic risk and resilience assessment of roadway networks in earthquake prone areas. *Bulletin of earthquake engineering*. 2019;17(1):181–210.
- [6] Lam C, Shimizu T. A network analytical framework to analyze infrastructure damage based on earthquake cascades: A study of earthquake cases in Japan. *International journal of disaster risk reduction*. 2021;54:102025.
- [7] Shao S, Huang X, Stanley HE, Havlin S. Percolation of localized attack on complex networks. *New Journal of Physics*. 2015;17(2):023049.
- [8] Berezin Y, Bashan A, Danziger MM, Li D, Havlin S. Localized attacks on spatially embedded networks with dependencies. *Scientific reports*. 2015;5(1):8934.
- [9] Vaknin D, Danziger MM, Havlin S. Spreading of localized attacks in spatial multiplex networks. *New Journal of Physics*. 2017;19(7):073037.
- [10] Dong G, Xiao H, Wang F, Du R, Shao S, Tian L, et al. Localized attack on networks with clustering. *New Journal of Physics*. 2019;21(1):013014.
- [11] Yan KS, Rong LL, Li Q. Vulnerability analysis of interdependent spatially embedded infrastructure networks under localized attack. *Modern Physics Letters B*. 2017;31(09):1750089.
- [12] Dong S, Gao X, Mostafavi A, Gao J. Modest flooding can trigger catastrophic road network collapse due to compound failure. *Communications Earth & Environment*. 2022;3(1):38.
- [13] Yuan X, Shao S, Stanley HE, Havlin S. How breadth of degree distribution influences network robustness: comparing localized and random attacks. *Physical Review E*. 2015;92(3):032122.
- [14] Vaknin D, Gross B, Buldyrev SV, Havlin S. Spreading of localized attacks on spatial multiplex networks with a community structure. *Physical Review Research*. 2020;2(4):043005.
- [15] Lv M, Pan L, Liu X. Cascading failures in interdependent directed networks under localized attacks. *Physica A: Statistical Mechanics and its Applications*. 2023;620:128761.
- [16] Geng H, Cao M, Guo C, Peng C, Du S, Yuan J. Global disassortative rewiring strategy for enhancing the robustness of scale-free networks against localized attack. *Physical Review E*. 2021;103(2):022313.
- [17] Fu T, Sun R, Li C, Wu L. Node differentiation protection concerning model of localized attack on real networks. *Physica A: Statistical Mechanics and its Applications*. 2019;526:120947.
- [18] Shang Y. Localized recovery of complex networks against failure. *Scientific reports*. 2016;6(1):30521.
- [19] Gong K, Wu JJ, Liu Y, Li Q, Liu RR, Tang M. The effective healing strategy against localized attacks on interdependent spatially embedded networks. *Complexity*. 2019;2019(1):7912857.
- [20] Chujo M, Liu S, Toriumi F. Improving network robustness against localized attacks by link modification. *Nonlinear Theory and Its Applications, IEICE*. 2025;16(3):561–572.
- [21] Hines P, Cotilla-Sanchez E, Blumsack S. Do topological models provide good information about electricity infrastructure vulnerability? *Chaos: An Interdisciplinary Journal of Nonlinear Science*. 2010;20(3).
- [22] Buldyrev SV, Parshani R, Paul G, Stanley HE, Havlin S. Catastrophic cascade of failures in interdependent networks. *Nature*. 2010;464(7291):1025–1028.
- [23] Zhou Y, Wang J, Sheu JB. On connectivity of post-earthquake road networks. *Transportation Research Part E: Logistics and Transportation Review*. 2019;123:1–16.
- [24] Wang W, Yang S, Stanley HE, Gao J. Local floods induce large-scale abrupt failures of road networks. *Nature communications*. 2019;10(1):2114.

[25] Artimo O, Grassia M, De Domenico M, Gleeson JP, Makse HA, Mangioni G, et al. Robustness and resilience of complex networks. *Nature Reviews Physics*. 2024;6(2):114–131.

[26] Schwarze AC, Jiang J, Wray J, Porter MA. Structural robustness and vulnerability of networks. *arXiv preprint arXiv:240907498*. 2024;.

[27] Albert R, Jeong H, Barabási AL. Error and attack tolerance of complex networks. *nature*. 2000;406(6794):378–382.

[28] Holme P, Kim BJ, Yoon CN, Han SK. Attack vulnerability of complex networks. *Physical review E*. 2002;65(5):056109.

[29] Morone F, Makse HA. Influence maximization in complex networks through optimal percolation. *Nature*. 2015;524(7563):65–68.

[30] Mugisha S, Zhou HJ. Identifying optimal targets of network attack by belief propagation. *Physical Review E*. 2016;94(1):012305.

[31] Grassia M, De Domenico M, Mangioni G. Machine learning dismantling and early-warning signals of disintegration in complex systems. *Nature communications*. 2021;12(1):5190.

[32] Ghanbari R, Jalili M, Yu X. Correlation of cascade failures and centrality measures in complex networks. *Future generation computer systems*. 2018;83:390–400.

[33] Xiao F, Li J, Wei B. Cascading failure analysis and critical node identification in complex networks. *Physica A: Statistical Mechanics and its Applications*. 2022;596:127117.

[34] Wang S, Liu W. Enhancing the robustness of influential seeds towards structural failures on competitive networks via a memetic algorithm. *Knowledge-Based Systems*. 2023;275:110677.

[35] Ou Z, Wang S. Finding robust and influential nodes on directed networks using a memetic algorithm. *Swarm and Evolutionary Computation*. 2024;87:101542.

[36] Schneider CM, Moreira AA, Andrade Jr JS, Havlin S, Herrmann HJ. Mitigation of malicious attacks on networks. *Proceedings of the National Academy of Sciences*. 2011;108(10):3838–3841.

[37] Barabási AL, Albert R. Emergence of scaling in random networks. *science*. 1999;286(5439):509–512.

[38] Freeman LC. Centrality in social networks conceptual clarification. *Social Networks*. 1978;1(3):215–239. doi:[https://doi.org/10.1016/0378-8733\(78\)90021-7](https://doi.org/10.1016/0378-8733(78)90021-7).

[39] Rossi RA, Ahmed NK. The Network Data Repository with Interactive Graph Analytics and Visualization. In: AAAI; 2015. Available from: <https://networkrepository.com>

[40] Colizza V, Pastor-Satorras R, Vespignani A. Reaction–diffusion processes and metapopulation models in heterogeneous networks. *Nature Physics*. 2007;3(4):276–282.

[41] Goh KI, Cusick ME, Valle D, Childs B, Vidal M, Barabási AL. The human disease network. *Proceedings of the National Academy of Sciences*. 2007;104(21):8685–8690.

[42] Rozemberczki B, Davies R, Sarkar R, Sutton C. GEMSEC: Graph Embedding with Self Clustering. In: Proceedings of the 2019 IEEE/ACM International Conference on Advances in Social Networks Analysis and Mining 2019. ACM; 2019. p. 65–72.

[43] Jeong H, Mason SP, Barabasi AL, Oltvai ZN. Lethality and centrality in protein networks. *arXiv preprint cond-mat/0105306*. 2001;.

[44] Opsahl T, Agneessens F, Skvoretz J. Node centrality in weighted networks: Generalizing degree and shortest paths. *Social networks*. 2010;32(3):245–251.

[45] Ficara A, Curreri F, Fiumara G, De Meo P. Human and social capital strategies for mafia network disruption. *IEEE Transactions on Information Forensics and Security*. 2023;18:1926–1936.